

Dissociation of Benzene Dication $[C_6H_6]^{2+}$: Exploring the Potential Energy Surface[†]

Smriti Anand[‡] and H. Bernhard Schlegel*

Department of Chemistry and Institute for Scientific Computing, Wayne State University, Detroit, Michigan 48202

Received: July 15, 2005; In Final Form: October 5, 2005

The singlet potential energy surface for the dissociation of benzene dication has been explored, and its three major dissociation channels have been studied: $C_6H_6^{2+} \rightarrow C_3H_3^+ + C_3H_3^+$, $C_4H_3^+ + C_2H_3^+$, and $C_5H_3^+ + CH_3^+$. The calculated energetics suggest that the products will be formed with considerable translational energy because of the Coulomb repulsion between the charged fragments. The calculated energy release in the three channels shows a qualitative agreement with the experimentally observed kinetic energy release. The formation of certain intermediates is found to be common to the three dissociation channels.

Introduction

Interaction of molecules with intense fields is a new and developing research area. These fields created by intense femtosecond lasers produce highly charged ions of molecules finally leading to Coulomb explosions. The energy release that accompanies this charge separation process is very large (typically 1–4 eV). The phenomenon of Coulomb explosion has been investigated in diatomic molecules and clusters, and studies have been extended to polyatomic molecules.^{1–31} Some of the molecules that have been studied are diatomics such as H_2 , N_2 , NO , I_2 , and CO , polyatomics such as SO_2 and CO_2 , and hydrocarbons such as acetylene, cyclopropane, butadiene, cyclohexane, benzene, toluene, and naphthalene. The Coulomb explosion of benzene is particularly interesting and has been studied extensively because of its high symmetry and diversity of dissociation pathways.^{27–37} The dissociation of benzene was studied, and its cation appearance energy was determined as early as 1938 by Hurstulid and co-workers.³⁸ Guilhaus et al.³⁹ studied the $[C_6H_6]^+$ ions formed via electron capture (EC) by $[C_6H_6]^{2+}$ and compared it to $[C_6H_6]^+$ ions generated by electron ionization (EI). The fragment abundance patterns for the ions formed by charge exchange were very similar to those for the singly charged ions generated by EI. Vékey and co-workers used the electron capture induced decomposition (ECID) method to study benzene dications.⁴⁰ Their study showed that only the ground-state ion participated in the EC process. The same authors used the ECID method to investigate the structures and isomers of $[C_6H_6]^{2+}$ ions formed by EI from benzene, 2,4-hexadiyne, and 1,5-hexadiyne and found significant differences among the isomers.⁴¹

Richardson and co-workers studied the charge separation reactions of doubly charged benzene ions using the photoion-photoion coincidence (PIPICO) technique.⁴² They observed three groups of ion pairs corresponding to $[C_3H_3]^+ + [C_3H_3]^+$, $[C_4H_3]^+ + [C_2H_3]^+$, and $[C_5H_3]^+ + [CH_3]^+$ and determined the kinetic energy release (KER) for each of the groups. Holland et al.³⁶ studied the latter charge separation channel and obtained a KER in very good agreement with the values reported by

Richardson et al. Bently and Wellington⁴³ used MINDO/3 semiempirical calculations to study the fragmentation energetics and charge distributions of benzene and isomeric dications. MINDO/3 calculations were also performed by Dewar and Holloway⁴⁴ on the benzene dication and its substituted derivatives. However, MINDO/3 calculations have been shown to be unsatisfactory for carbodication energetics.⁴⁵ Lammertsma and Schleyer⁴⁵ studied the structures and energetics of $[C_6H_6]^{2+}$ isomers and their fragmentation into $[C_5H_3]^+ + [CH_3]^+$ by ab initio methods. Krogh-Jespersen⁴⁶ carried out ab initio molecular orbital calculations on a series of $[C_6H_6]^{2+}$ isomers to investigate the singlet and triplet surfaces. Recently, Zyubina and others have performed density functional theory (DFT) calculations to study the dissociation pathways of the benzene trication.^{47,48} However, no similar study of the barriers and reaction pathways for the dication has been reported. The structures and energetics of $C_3H_3^+$ ions have been investigated by Lammertsma et al.,⁴⁵ Zerner and co-workers,⁴⁹ and Kompe et al.⁵⁰ The isomers of $C_4H_3^+$ have been examined recently in combined experimental and computational studies.^{51,52} The structures of $C_3H_3^+$ cations are well-known experimentally and have been calculated by Zerner and co-workers.⁵³

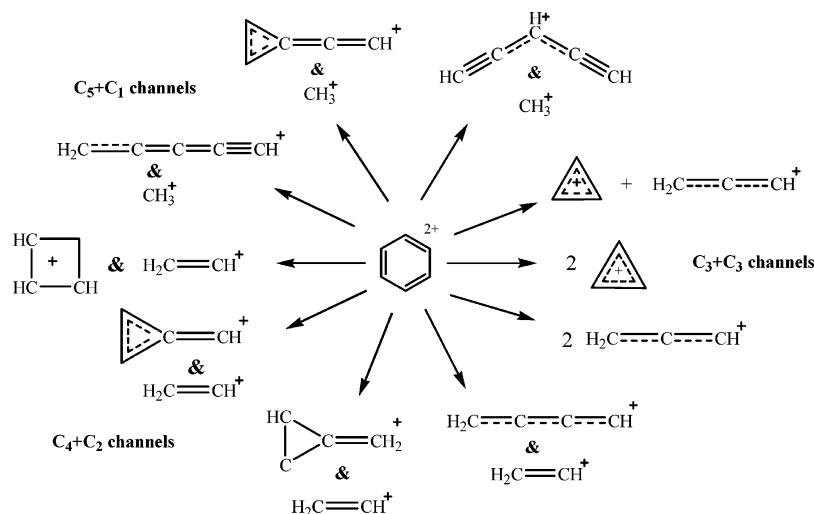
The present study aims to explore the singlet potential energy surface (PES) for the dissociation of the benzene dication. In particular, the reaction pathways, intermediates, and transition structures for the three major channels will be characterized. Another goal of the study is to establish the level of theory needed for an ab initio molecular dynamics investigation of benzene dication dissociation. During the excitation and dissociation, it is possible for benzene dication and the product fragments to be formed in either the singlet or triplet state. The separation between the singlet and triplet in the parent dication was found to be about 5 kcal/mol in an earlier study.⁴⁶ However, the most stable $C_3H_3^+$ and $C_5H_3^+$ fragments are found to be singlet ions with the triplet ions being about 30–50 kcal/mol higher in energy.^{49,53} Because the kinetic energy release observed in the three channels during the dissociation process is ~70–100 kcal/mol, it is anticipated that the fragments are formed in the singlet state. Preliminary calculations at the B3LYP level of theory suggest that the lowest energy triplet products in the C_3+C_3 , C_2+C_4 , and C_5+C_1 channels are, respectively, about 200, 70, and 147 kcal/mol higher than the

[†] Part of the special issue "Jack Simons Festschrift".

* Corresponding author. E-mail: hbs@chem.wayne.edu.

[‡] Current address: Christopher Newport University, Newport News, VA 23606.

SCHEME 1



corresponding singlet products and, hence, only the singlet PES is considered.

Methods

The electronic structure calculations were carried out using the development version of the Gaussian series of programs.⁵⁴ The structures of the reactant dication, product cations, potential intermediates, and transition states were optimized by Hartree–Fock, second-order Møller–Plesset perturbation theory, and B3LYP^{55,56} density functional theory with the 3-21G, 6-31G(d), and 6-311+G(d) basis sets. The CBS-QB3 and CBS-APNO complete basis set methods of Petersson and co-workers^{57,58} were used to compute accurate heats of reaction. The QST2/QST3 method⁵⁹ was used to search for some of the transition states (TS) involved in the dissociation process. All of the TSs were checked by a frequency calculation, and selected TSs were verified with reaction path following methods.^{60–62}

Results and Discussion

The major product channels for the dissociation of benzene dication are presented in Scheme 1.

The different products can be grouped into the three major dissociation channels observed by Richardson and co-workers: C_3+C_3 , C_4+C_2 , and C_5+C_1 . The dissociation mechanisms for these channels are discussed below in detail. The structures of the reactant ion, various product fragments, intermediates, and transition states involved in the dissociation are presented in Figures 1–3. The heats of reaction for the different dissociation pathways are collected in Table 1. The energetics at the HF level have a mean absolute deviation (MAD) of ~ 10 – 12 kcal/mol relative to our most accurate values obtained at the CBS-APNO level of theory. The B3LYP energies have a MAD of 2–2.6 kcal/mol compared to the CBS-APNO data, whereas the MP2 energies have a MAD of 4.8–5.7 kcal/mol.

Isomerization and fragmentation occurs via a network of reactions. Ring opening leads to a linear six-carbon system. The various structural isomers of the linear chain can be enumerated systematically, and at least a dozen are relevant to the dissociation mechanism. These are interrelated by 1,2, 1,3, and 1,4 hydrogen shifts. Ring closure and/or bond breaking in a few of these isomers leads to the dissociation products. The intermediates may have several conformations and some may prefer nonclassical structures with bridging hydrogens. However, these energy differences should be smaller than the barriers for ring

opening of benzene dication and most of the isomerization reactions. In the following sections we discuss the structure of the reactant and various pathways to the low energy products of the C_3+C_3 , C_4+C_2 , and C_5+C_1 channels. Because of the large number of intermediates and transition states, it was not practical to calculate these at the CBS level of theory. Calculations were carried out with B3LYP and MP2 methods with a number of basis sets. The relative energies at the various levels of theory are collected in Tables 1–3. Because B3LYP calculations tend to underestimate the barrier heights, most of the discussion is based on the MP2/6-311+G(d) energies.

Reactant. The most stable benzene-like structure of the singlet benzene dication is the chair conformation (structure **R1** in Figure 1), which belongs to the C_{2h} point group. Two other

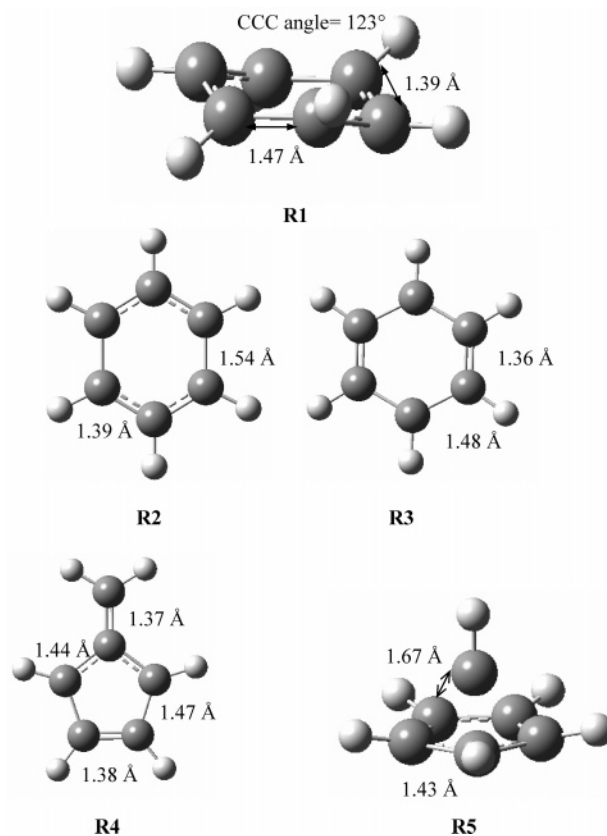


Figure 1. Minima on the benzene dication potential energy surface.

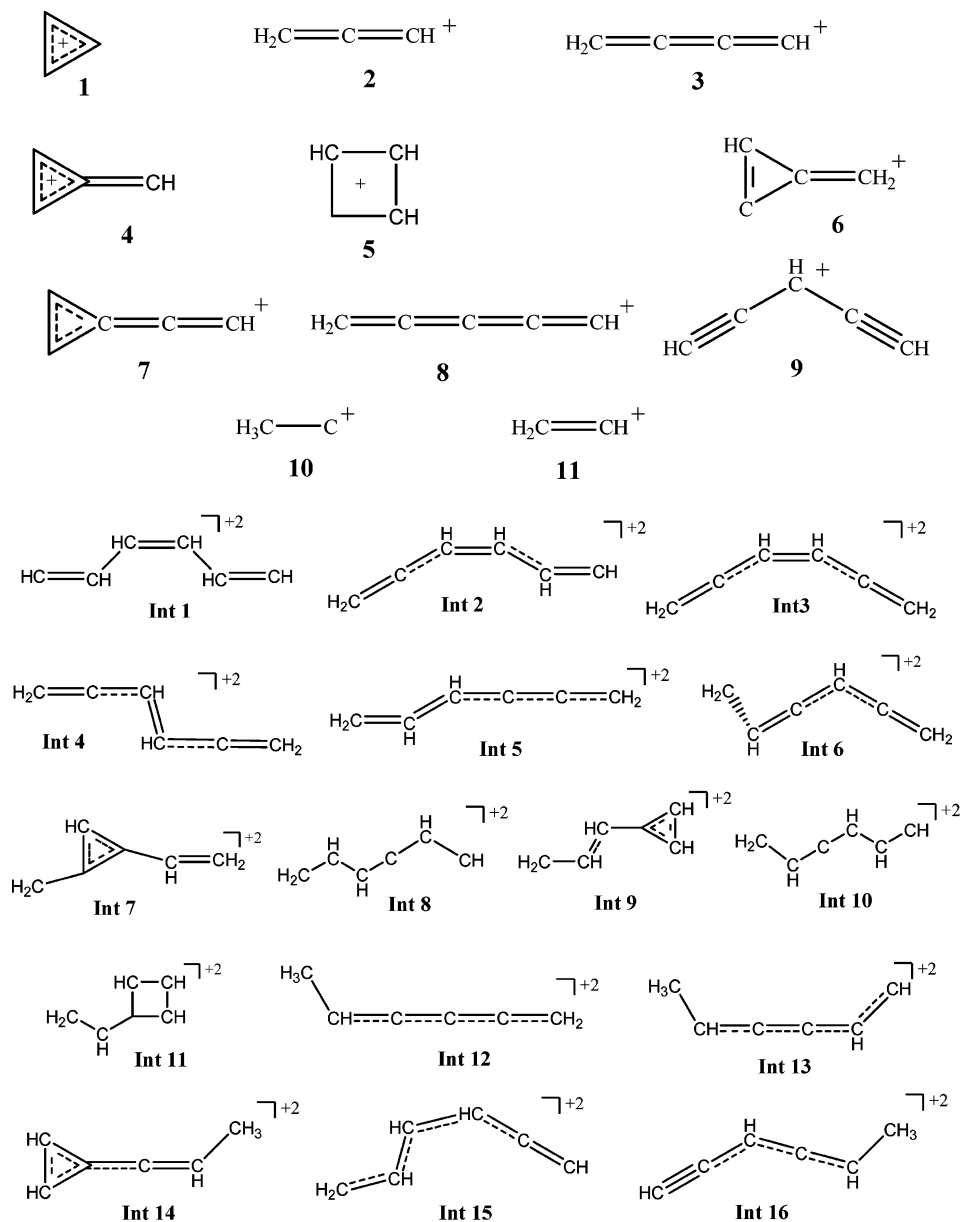


Figure 2. Structures of the products and intermediates in the dissociation of benzene dication (see Figures 4–6 for the potential energy profiles).

TABLE 1: Heats of Reaction for the Dissociation of Benzene Dication^a

| reaction | HF/ 6-31G(d) | HF/ 6-311+G(d) | B3LYP/ 6-31G(d) | B3LYP/ 6-311+G(d) | MP2/ 6-31G(d) | MP2/ 6-311+G(d) | CBS- QB3 | CBS- APNO |
|--|-----------------|-------------------|--------------------|----------------------|------------------|--------------------|-------------|--------------|
| C₃ + C₃ channel | | | | | | | | |
| R1 1 + 1 | -92.04 | -91.06 | -69.76 | -70.43 | -77.08 | -74.49 | -72.90 | -72.32 |
| R1 1 + 2 | -58.16 | -58.70 | -44.01 | -46.61 | -45.19 | -44.33 | -45.28 | -45.00 |
| R1 2 + 2 | -24.27 | -26.34 | -18.26 | -22.79 | -13.30 | -14.18 | -17.67 | -17.68 |
| C₄ + C₂ channel | | | | | | | | |
| R1 3 + 10 | 24.84 | 22.67 | 31.81 | 27.34 | 42.07 | 40.63 | 32.90 | 32.90 |
| R1 3 + 11 | -15.35 | -17.22 | -12.79 | -17.99 | -4.79 | -5.83 | -12.65 | -12.47 |
| R1 4 + 10 | 41.64 | 40.49 | 53.01 | 49.84 | 59.29 | 57.78 | 50.07 | 50.28 |
| R1 4 + 11 | 1.45 | 0.60 | 8.42 | 4.52 | 12.43 | 11.32 | 4.52 | 4.92 |
| R1 5 + 10 | 44.95 | 42.70 | 63.11 | 61.52 | 67.24 | 65.58 | 59.43 | 60.16 |
| R1 5 + 11 | 4.76 | 2.81 | 18.51 | 16.19 | 20.37 | 19.12 | 13.88 | 14.79 |
| R1 6 + 10 | 54.94 | 52.97 | 64.12 | 61.74 | 72.56 | 71.20 | 62.47 | 62.84 |
| R1 6 + 11 | 14.75 | 13.08 | 19.52 | 16.42 | 25.70 | 24.74 | 16.92 | 17.48 |
| C₅ + C₁ channel | | | | | | | | |
| R1 7 + CH₃ | -33.21 | -35.01 | -11.56 | -15.06 | -18.40 | -18.80 | -16.35 | -15.16 |
| R1 8 + CH₃ | -9.52 | -12.70 | -1.85 | -7.14 | 1.75 | -1.79 | -0.96 | -0.36 |
| R1 9 + CH₃ | -6.65 | -9.68 | 4.99 | -0.38 | 3.12 | 0.77 | 2.75 | 3.55 |
| RMS error^b | 10.96 | 12.37 | 2.31 | 3.40 | 6.44 | 5.43 | 0.59 | |
| MAD^b | 9.70 | 11.38 | 2.02 | 2.59 | 5.65 | 4.84 | 0.49 | |

^a Enthalpies at 298 K in kcal/mol relative to the reactant (see Figures 1 and 2 for the structure numbers). ^b The RMS error and MAD is relative to CBS-APNO.

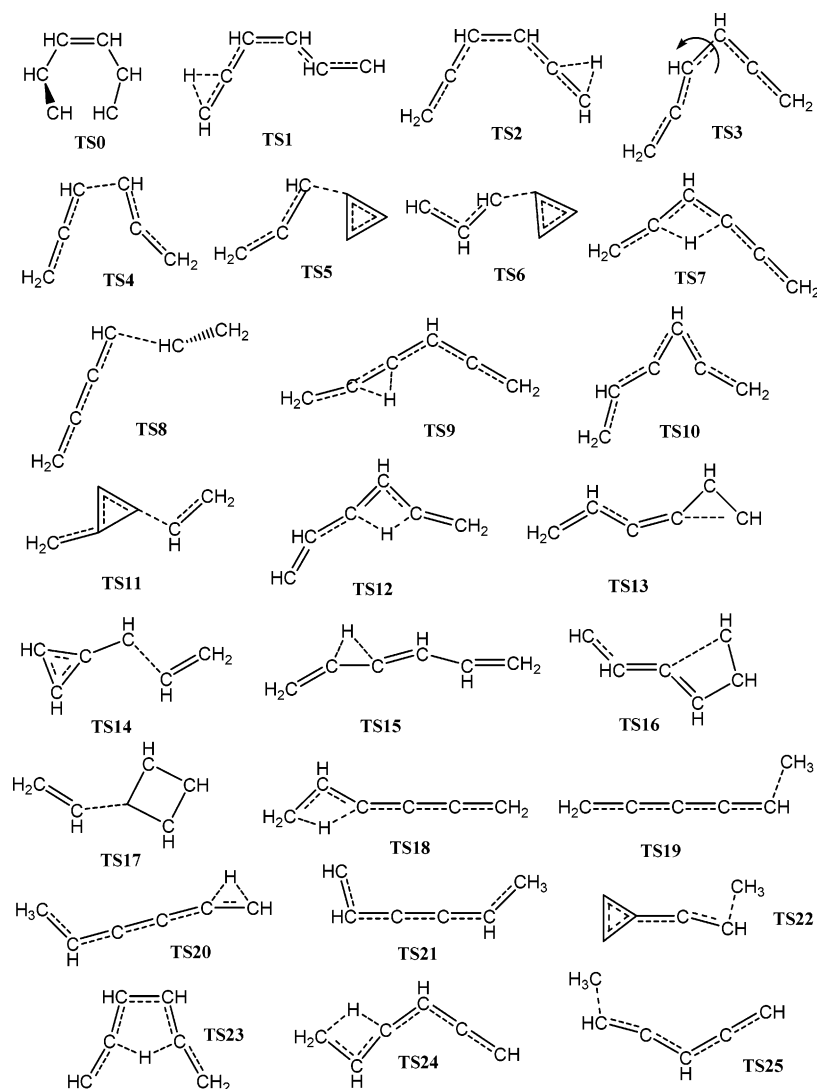


Figure 3. Structures of the transition states in the dissociation of benzene dication (see Figures 4–6 for the potential energy profiles). All of the structures are doubly charged.

TABLE 2: Energies of Intermediates Involved in the Dissociation of Benzene Dication^a

| intermediates | HF/ 6-31G(d) | HF/ 6-311+G(d) | B3LYP/ 6-31G(d) | B3LYP/ 6-311+G(d) | MP2/ 6-31G(d) | MP2/ 6-311+G(d) |
|---------------|-----------------|-------------------|--------------------|----------------------|-------------------|--------------------|
| Int1 | 45.81 | 45.03 | 52.35 | 48.76 | 39.57 | 36.86 |
| Int2 | 29.81 | 29.10 | 31.23 | 28.53 | 33.11 | 31.44 |
| Int3 | 23.18 | 22.44 | 19.84 | 17.38 | 32.87 | 32.22 |
| Int4 | 17.53 | 16.96 | 15.51 | 13.26 | 28.07 | 27.77 |
| Int5 | 0.21 | -0.66 | 1.64 | -0.28 | 10.92 | 10.53 |
| Int6 | 13.19 | 12.46 | 13.01 | 16.77 | 21.94 | 21.52 |
| Int7 | 16.73 | 17.01 | 19.27 | 18.90 | 24.80 | 25.00 |
| Int8 | 65.75 | 65.09 | 74.26 ^b | 71.91 ^b | 89.8 ^b | 89.38 ^b |
| Int9 | -21.58 | -21.27 | -8.49 | -8.92 | -10.21 | -9.07 |
| Int10 | 27.47 | 26.65 | 29.61 | 26.89 | 21.94 | 21.59 |
| Int11 | -5.97 | -6.41 | 0.56 | 0.69 | 0.56 | 0.69 |
| Int12 | 14.78 | 13.31 | 6.86 | 4.02 | 25.65 | 23.88 |
| Int13 | 38.81 | 37.16 | 39.17 | 34.71 | 35.88 | 32.05 |
| Int14 | 12.49 | 12.18 | 14.67 | 13.44 | 22.65 | 22.88 |
| Int15 | 14.86 | 14.10 | 18.69 | 16.69 | 22.50 | 21.95 |
| Int16 | 44.51 | 43.16 | 38.51 | 35.52 | 51.21 | 49.82 |

^a Enthalpies at 298 K in kcal/mol relative to the reactant (see Figure 2 for the structure labels). ^b Single point calculations at HF/6-311+G(d) optimized geometry.

planar structures, **R2** and **R3**, are about 9 and 12 kcal/mol, respectively, higher in energy than **R1** at the MP2/6-311+G(d) level of theory. Both **R2** and **R3** are of D_{2h} symmetry and have one and two imaginary frequencies, respectively. Fulvene dication, **R4**, and the pyramidal structure, **R5**, are, respectively,

~1 and 16 kcal/mol lower than the **R1** benzene dication at the CBS-QB3 level of theory. In previous studies, the pyramidal dication was found to be the global minimum on the singlet PES.⁴⁶ Double ionization of benzene should initially form benzene dication **R1** rather than **R4** or **R5**. Hence, the

TABLE 3: Energies of the Transition States in the Dissociation of Benzene Dication^a

| transition State | HF/ 6-31G(d) | HF/ 6-311+G(d) | B3LYP/ 6-31G(d) | B3LYP/ 6-311+G(d) | MP2/ 6-31G(d) | MP2/ 6-311+G(d) |
|------------------|-----------------|-------------------|--------------------|----------------------|--------------------|--------------------|
| TS0 | 61.20 | 60.56 | 57.48 | 55.05 | 54.80 | 52.92 |
| TS1 | 48.33 | 46.82 | 51.58 | 47.78 | 48.95 | 46.51 |
| TS2 | 34.53 | 32.93 | 32.47 | 31.03 | 33.98 | 32.64 |
| TS3 | 48.11 | 47.39 | 40.45 | 39.01 | 48.30 | 47.28 |
| TS4 | 70.39 | 68.38 | 59.12 | 55.83 | 70.80 | 65.36 |
| TS5 | 88.23 | 86.64 | 59.73 | 58.26 | 63.91 | 62.40 |
| TS6 | 96.30 | 95.06 | 80.52 | 79.92 | 66.96 | 65.71 |
| TS7 | 69.42 | 67.73 | 53.84 | 51.91 | 67.72 | 65.86 |
| TS8 | 61.94 | 60.59 | 55.97 | 51.87 | 69.02 | 66.53 |
| TS9 | 47.09 | 44.89 | 35.05 | 31.92 | 47.47 | 45.41 |
| TS10 | 30.77 | 30.09 | 22.24 | 21.11 | 29.19 | 28.38 |
| TS11 | 67.78 | 66.72 | 72.65 | 70.01 | 79.55 | 78.25 |
| TS12 | 99.92 | 98.09 | 91.38 | 88.80 | 108.9 ^b | 107.3 ^b |
| TS13 | 68.97 | 68.00 | 68.49 | 66.15 | 84.89 | 84.20 ^c |
| TS14 | 61.83 | 61.02 | 72.09 | 69.11 | 81.11 | 79.79 |
| TS15 | 61.43 | 59.50 | 54.78 | 51.21 | 45.89 | 44.00 |
| TS16 | 40.91 | 39.74 | 37.75 | 36.00 | 38.80 | 37.31 |
| TS17 | 59.49 | 58.05 | 72.74 | 70.63 | 73.85 | 72.00 |
| TS18 | 54.52 | 52.17 | 45.72 | 43.16 | 53.98 | 51.93 |
| TS19 | 51.45 | 48.63 | 54.09 | 49.24 | 63.08 | 60.25 |
| TS20 | 42.92 | 40.35 | 35.41 | 31.03 | 36.62 | 34.11 |
| TS21 | 43.06 | 41.29 | 41.82 | 38.49 | 48.30 | 46.68 |
| TS22 | 29.79 | 28.60 | 45.91 | 42.68 | 41.94 | 41.14 |
| TS23 | 65.62 | 63.94 | 47.41 | 44.98 | 52.31 | 47.49 |
| TS24 | 64.07 | 66.72 | 54.64 | 52.05 | 57.43 | 55.30 |
| TS25 | 62.66 | 60.41 | 67.52 | 62.49 | 69.50 | 66.82 |

^a Enthalpies at 298 K in kcal/mol relative to the reactant (see Figure 3 for the structure labels). ^b Single point calculations at HF/6-311+G(d) optimized geometry. ^c MP2/6-311+G(d) single point calculation at MP2/6-31G(d) optimized geometry.

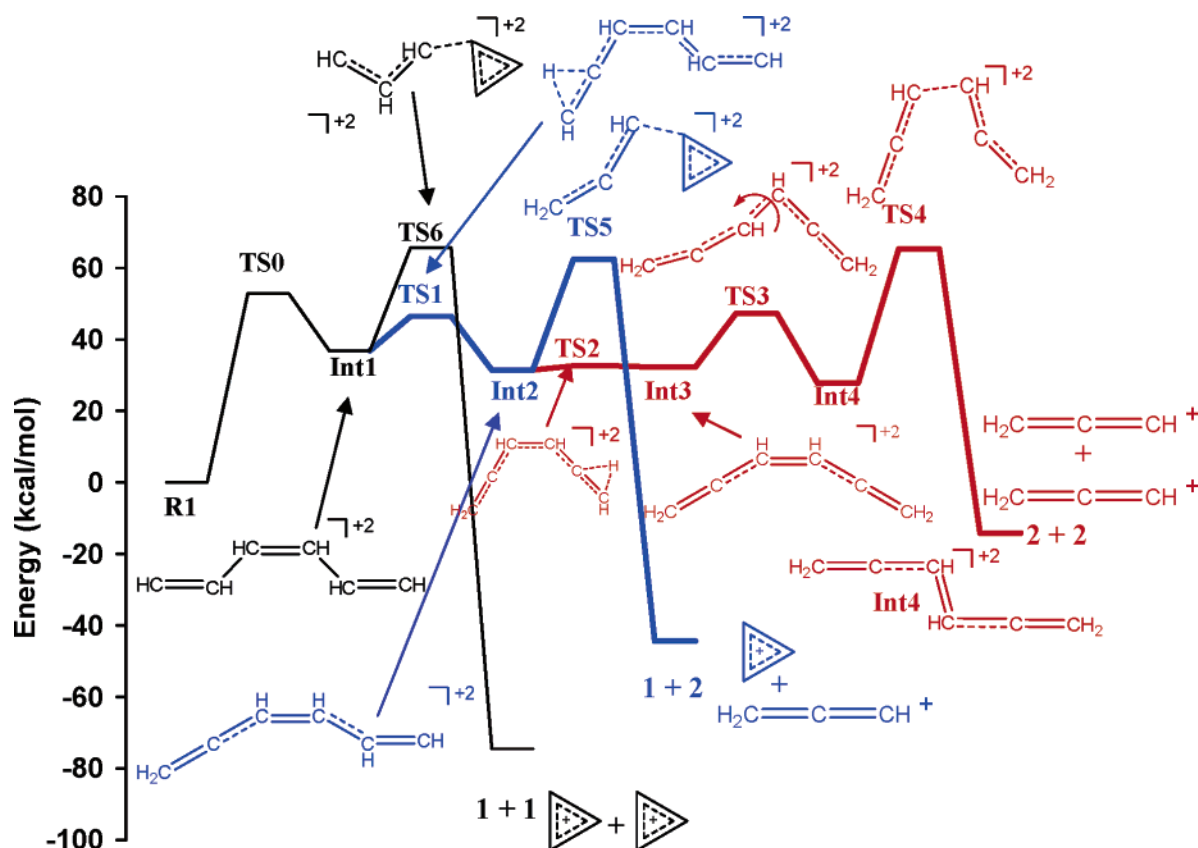


Figure 4. Potential energy profile along the $[C_3H_3]^+ + [C_3H_3]^+$ dissociation channel of benzene dication at the MP2/6-311+G(d) level of theory.

isomerization and fragmentation pathways for benzene dication investigated in the present study were started from the ring opening of **R1**. Isomerization to **R4** or **R5** could occur via one or more of the ring-opened intermediates.

$C_3 + C_3$ Channel: $[C_6H_6]^{2+} \rightarrow [C_3H_3]^+ + [C_3H_3]^+$. Of the possible isomers of $C_3H_3^+$, the most stable is the cyclopropenyl

cation (**1**). This is expected because of its aromatic character. The 2-propynyl cation (**2**) is 27 kcal/mol above **1** at the CBS-APNO level. Other isomers have been found to be much higher in energy.⁵³ Thus, for the $[C_6H_6]^{2+} \rightarrow [C_3H_3]^+ + [C_3H_3]^+$ reaction, the product channels **1 + 1**, **1 + 2**, and **2 + 2** are likely to occur most frequently. The PES along this dissociation

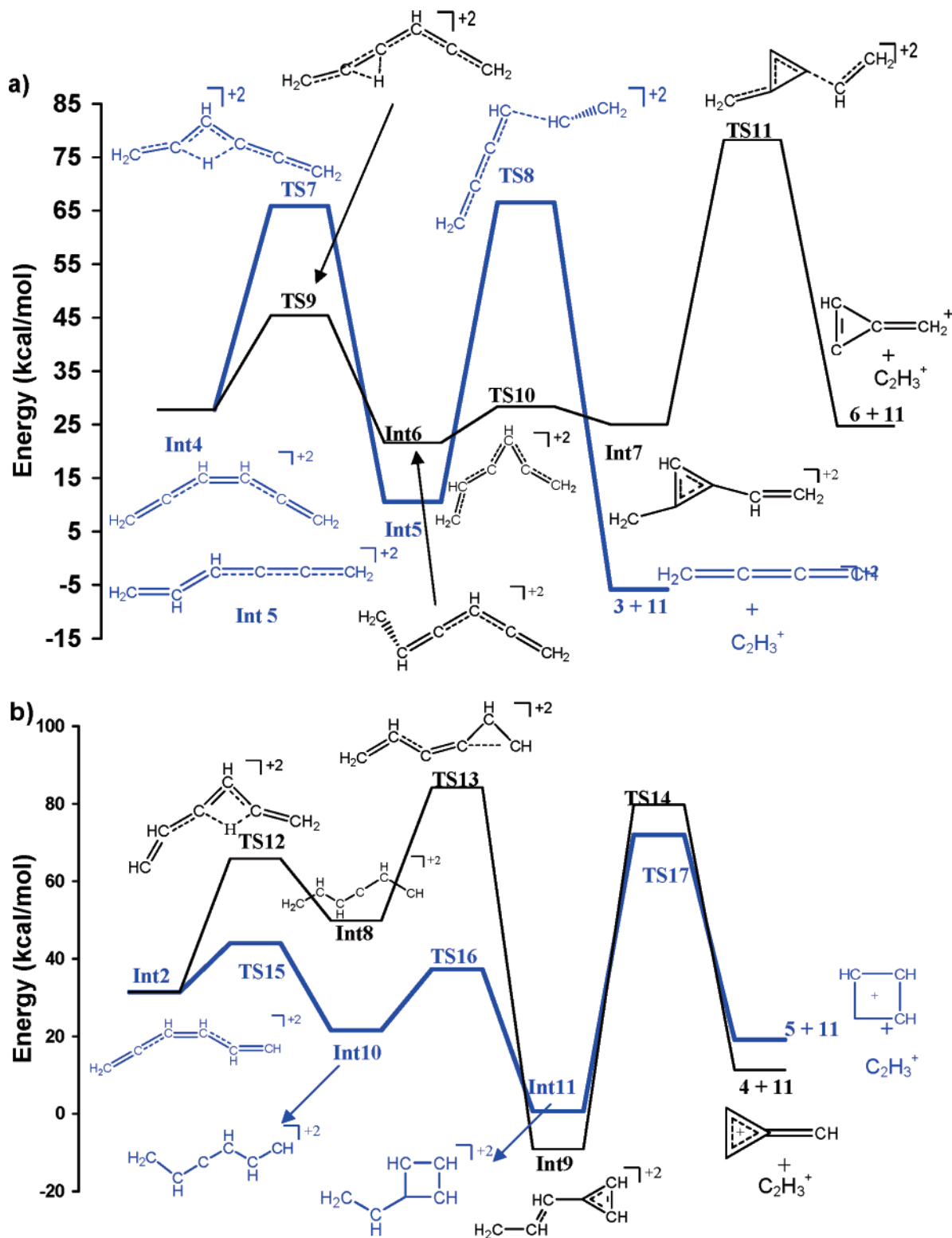


Figure 5. Potential energy profile along the $[C_4H_3]^+ + [C_2H_3]^+$ dissociation channel of benzene dication at the MP2/6-311+G(d) level of theory. (a) The 3 + 11 and 6 + 11 channels starting from Int4 in Figure 4. (b) The 4 + 11 and 5 + 11 channels starting from Int2 in Figure 4.

channel at the MP2/6-311+G(d) level of theory is presented in Figure 4. All of the dissociation pathways begin with ring opening of the benzene dication via TS0. This leads to Int1 and involves a barrier of about 53 kcal/mol. Intermediate Int2 is formed from Int1 by a 1,2 hydrogen transfer via transition state TS1 and is followed by formation of Int3 by a second hydrogen transfer via TS2. These hydrogen-transfer transition states are about 15 and 0.4 kcal/mol above intermediates Int1 and Int2, respectively. Addition of p functions on the hydrogens

via the 6-311+G(d,p) basis set lowered TS1 by only 2 kcal/mol. Other transition states involving 1,3 and 1,4 hydrogen shifts also showed a lowering of the barrier by about 2–4 kcal/mol. Intermediate Int3 can then isomerize to Int4 by rotating about the central bond via TS3. This intermediate, Int4, can subsequently dissociate by rupture of the central C–C bond via TS4 to form two 2-propynyl cations, 2 + 2. Transition state TS3 is about 15 kcal/mol above Int3 and TS4 is 38 kcal/mol above Int4. Intermediate Int2 can also form 1 + 2 via transition state

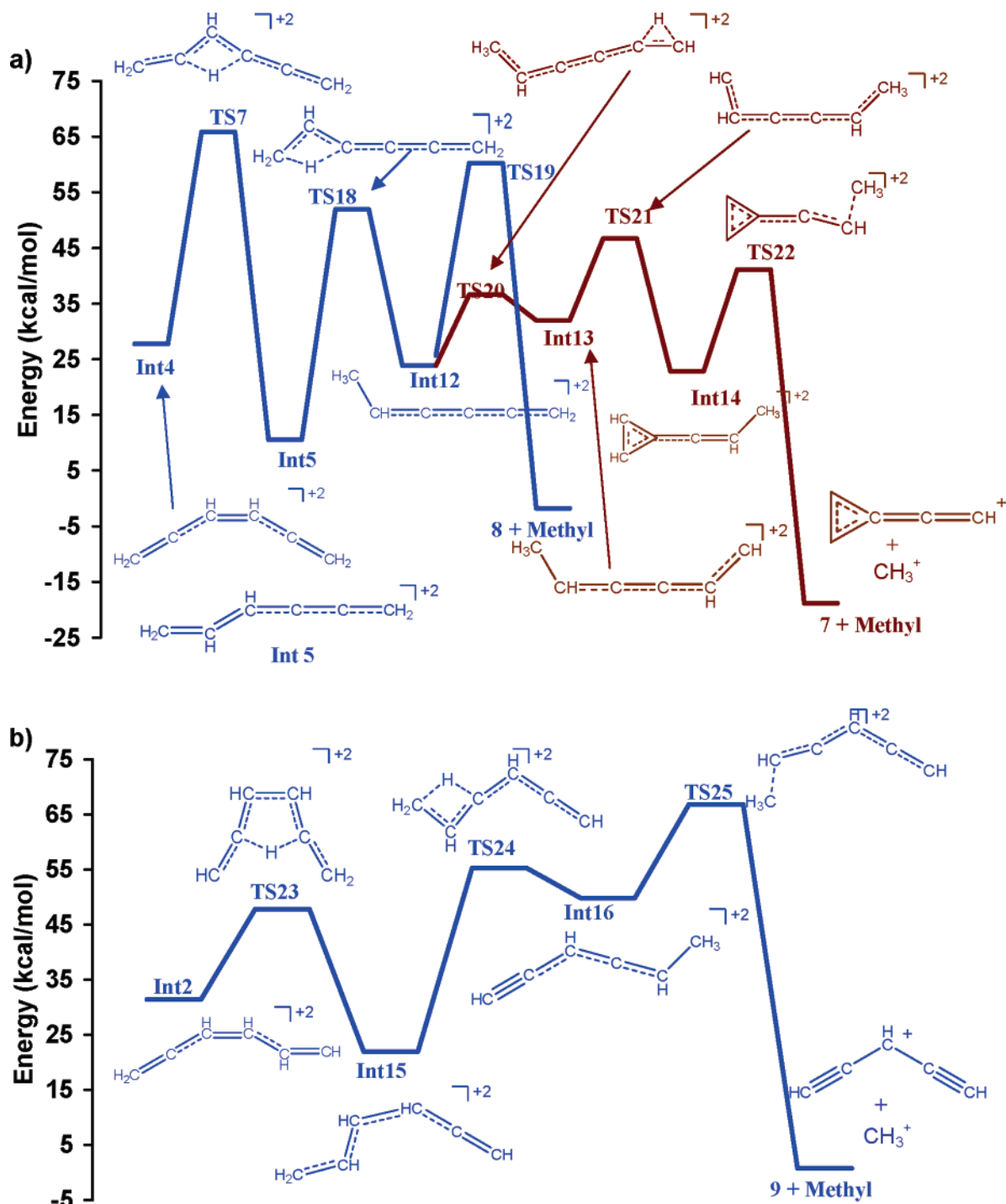


Figure 6. Potential energy profile along the $[C_5H_3]^+ + [CH_3]^+$ dissociation channel of benzene dication at the MP2/6-311+G(d) level of theory. (a) The 6 + methyl and 7 + methyl channels starting from **Int4** in Figure 4. (b) The 9 + methyl channel starting from **Int2** in Figure 4.

TS5 (lying about 31 kcal/mol above **Int2**). Formation of two cyclopropenyl cations follows the path **Int1** \rightarrow **TS6** \rightarrow **1** + **1**, and the barrier for this process is about 29 kcal/mol relative to **Int1**. The reaction path following from **TS5** and **TS6** indicates that no other intermediate is involved in the formation of the products (**1** + **2** and **1** + **1**) or in the formation of the transition states from the respective reactants, **Int1** and **Int2**. The energy release on going from the final transition states (**TS4**, **TS5**, and **TS6**) to the three products of the $C_3 + C_3$ channel is in the range of 80–140 kcal/mol. A considerable portion of this energy should appear as translational kinetic energy of the products as a result of the Coulomb repulsion between the product ions.

$C_4 + C_2$ Channel: $[C_6H_6]^{2+} \rightarrow [C_4H_3]^+ + [C_2H_3]^+$. The 2-propynylmethyl cation (**3**), methylmethyl-2-cyclopropen-1-ylidene ion (**4**), 1,3-cyclobutadien-1-ylmethyl cation (**5**), and 1-cyclopropen-1-ylmethyl-3-methylene cation (**6**) are the lowest energy isomers of the C_4H_3 ion. Structures **4**, **5**, and **6** are, respectively, 17, 27, and 30 kcal/mol higher in energy than **3** at the CBS-APNO level. The delocalization of the charge over the cumulative π system accounts for the stability of **3**. For the C_2H_3 ion, the 1-ethynyl-1-ylidene cation (**10**) and the ethynylmethyl cation (**11**) are the two stable isomers with **11** being 45 kcal/mol lower in energy than **10**. Structure **11** is the protonated form of acetylene, and the charge is delocalized over both carbon

atoms and accounts for its greater stability. Higher levels of theory such as CBS-APNO find the nonclassical structure of protonated acetylene to be ~ 4 kcal/mol lower than the classical form. For other structures, higher level calculations may also reveal some nonclassical structures a few kcal/mol lower in energy.

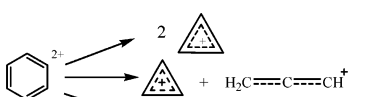
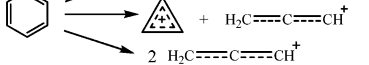
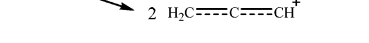
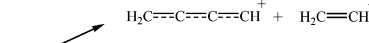
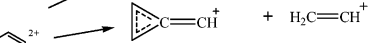
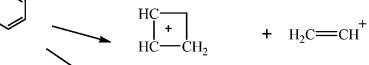
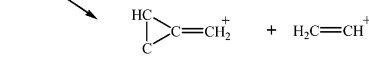
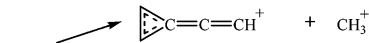
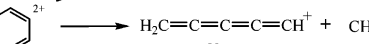
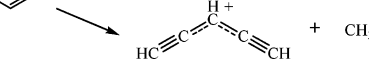
The pathway to **3** and **6** starts with **Int4** as shown in Figure 5a at the MP2/6-311+G(d) level. The formation of **Int5** from **Int4** involves a hydrogen transfer proceeding via **TS7**, which lies 38 kcal/mol above **Int4**. Products **3** + **11** can be formed from **Int5** by C–C bond dissociation via **TS8**, which is about 56 kcal/mol higher in energy relative to **Int5**. Intermediate **Int4** can also form **Int6** via **TS9**, and the barrier for this process is ~ 24 kcal/mol relative to **Int4**. The cyclization of **Int6** to **Int7** involves **TS10**, which lies 7 kcal/mol above **Int6**. Intermediate **Int7** can then dissociate to form products **6** + **11** via transition state **TS11**. Products **4** and **5** are formed starting from **Int2** (Figure 5b). A 1,3 hydrogen shift in **Int2** leads to **Int8**, which is stable at the Hartree–Fock level but unstable at the B3LYP and MP2 levels. Attempts to optimize **Int8** at the MP2 level lead to **Int5**. A ring closure in **Int8** results in the formation of **Int9** from which a C–C bond fission leads to products **4** + **11**. **Int2** can also undergo a 1,2 hydrogen shift to form **Int10** via **TS14**. From **Int10**, **Int11** is formed by cyclization. Products **5** + **11** are then formed from **Int11** via a C–C bond dissociation. However, the barriers for these C–C bond dissociations are very high and, hence, formation of **4** + **11** and **5** + **11** seems to be less likely. From the data in Table 1, one can see that reactions involving the formation of **3** + **11** are about 17–75 kcal/mol more exothermic than the other **C**₄ + **C**₂ products listed. Also, the best **C**₄ + **C**₂ channel is less exothermic by 5–60 kcal/mol than the three **C**₃ + **C**₃ channels. For these dissociation channels, the energy release on going from the final transition states to the products is ca. 54–72 kcal/mol.

C₅ + **C**₁ Channel: $[C_6H_6]^{2+} \rightarrow [C_5H_3]^+ + [CH_3]^+$. The lowest energy isomers of the **C**_{5**H**₃ ion are the cyclopropenylum ethynyl cation (**7**), the 2-propynylum,1-ethynyl cation (**8**), and the 1,2,3,4-pentatetraenylum cation (**9**). This is in agreement with previous calculations.^{45,49,50} Structures **8** and **9** are, respectively, 15 and 19 kcal/mol higher in energy than **7** at the CBS-APNO level. The stability of **7** can be attributed to the presence of the three-membered ring in conjugation with the remaining carbon atoms. Figure 6 shows the PES along this dissociation channel at the MP2/6-311+G(d) level. Intermediate **Int5** can be formed from **Int4** by a 1,3 hydrogen shift via **TS7**. A second 1,3 shift (in **Int5**) can then form **Int12** via transition state **TS18** and a barrier of 41 kcal/mol relative to **Int5** (see Figure 6a). Both of these barriers (**TS7** and **TS18**) are lowered by about 3 kcal/mol when p functions were added to the hydrogens. Dissociation along the C–CH₃ bond in **Int12** results in the formation of products **8** + methyl cation. Intermediate **Int12** can also form intermediate **Int13** via a hydrogen transfer proceeding through **TS20**. Cyclization of **Int13**, proceeding through **TS21** (lying about 15 kcal/mol above **Int13**), results in the formation of intermediate **Int14**. Loss of the methyl cation from **Int14** leads to products **7** + methyl cation. As seen from Figure 6b, a 1,4 H transfer from **Int2** results in **Int15** via **TS23**. A 1,3 hydrogen transfer in **Int15** converts it to **Int16** via **TS24**. Cleavage of the C–CH₃ bond in **Int16** results in the formation of products **9** + methyl cation proceeding via **TS25**. The product channel **7** + methyl cation is more exothermic than the other two product channels (by 15–19 kcal/mol). The energy release in this **C**₅+**C**₁ channel is about 60 kcal/mol.}

Conclusions

In this study, the three major dissociation channels of benzene dication have been investigated. The heats of reaction calculated at the B3LYP level agree better with the CBS results than do the MP2 calculations. However, as is frequently found, the B3LYP barriers tend to be a bit lower than the MP2 barriers. The Hartree–Fock results are less satisfactory than either the B3LYP or MP2 calculations. This suggests that an initial survey of the dynamics of benzene dication dissociation by ab initio classical trajectory calculations could be carried out with density functional theory and perhaps selected cases should be followed up by MP2 trajectory calculations.

The energy release on dissociation can be estimated as the difference between the last transition state and the product. The calculated values for the three channels are 80–140 kcal/mol, 68–72 kcal/mol, and 60–66 kcal/mol and follows the order $[C_3H_3]^+ + [C_3H_3]^+ > [C_4H_3]^+ + [C_2H_3]^+ > [C_5H_3]^+ + [CH_3]^+$. This is in qualitative agreement with the experimental kinetic energy release of 4.2 eV (96 kcal/mol), 3.8 eV (87 kcal/mol), and 3.0 eV (69 kcal/mol) for the **C**₃+**C**₃, **C**₄+**C**₂, and **C**₅+**C**₁ dissociation channels, respectively. All of the products are expected to be formed with considerable translational energy resulting from the Coulomb repulsion between the charged fragments. The energy releases, heats of reaction, and barrier heights (in kcal/mol computed at the MP2/6-311+G(d) level of theory) for the three channels are summarized below.

| | ΔH_{rxn} | ΔH^\ddagger | $\Delta H_{release}$ |
|--|------------------|---------------------|----------------------|
| C ₃ + C ₃ channel (See Figure 4) | | | |
|  | -74.5 | 65.7 | 140.2 |
|  | -44.3 | 62.4 | 106.7 |
|  | -14.2 | 65.4 | 79.6 |
| C ₄ + C ₂ channel (See Figure 5) | | | |
|  | -5.8 | 66.5 | 72.3 |
|  | 11.3 | 79.9 | 68.6 |
|  | 19.1 | 72.0 | 52.9 |
|  | 24.7 | 78.2 | 53.5 |
| C ₅ + C ₁ channel (See Figure 6) | | | |
|  | -18.8 | 41.4 | 60.2 |
|  | -1.8 | 60.2 | 62.0 |
|  | 0.77 | 66.8 | 66.0 |

The fragmentation in the parent ion involves breaking the cyclic structure, hydrogen transfers, and skeletal rearrangements. The initial pathway leading to the formation of **Int2** is common to the **1** + **2**, **2** + **2**, **9** + methyl, **4** + **11**, and **5** + **11** dissociation reactions. In the **7** + methyl, **8** + methyl, and the two **C**₄+**C**₂ channels (**3** + **11** and **6** + **11**), the commonality is the dissociation leading to **Int4**. The current study has explored the pathways for dissociation that appear to be the most feasible. Other intermediates and lower energy dissociation pathways may exist, but diligent searching has not yet revealed them. In the future, the dissociation will be studied using ab initio molecular dynamics to gain further insight into the fragmentation process.

Acknowledgment. A grant from the National Science Foundation (CHE 0512144) supported this work. We are

thankful to C&IT and ISC (at Wayne State University) for the computer time made available.

Supporting Information Available: Cartesian coordinates and B3LYP/6-31G(d) total energies are listed for each molecule. This material is available free of charge via the Internet at <http://pubs.acs.org>.

References and Notes

- (1) Zavriyev, A.; Bucksbaum, P. H.; Muller, H. G.; Schumacher, D. W. *Phys. Rev. A* **1990**, *42*, 5500–5513.
- (2) Chelkowski, S.; Bandrauk, A. D. *J. Phys. B* **1995**, *28*, L723–L731.
- (3) Cornaggia, C.; Schmidt, M.; Normand, D. *Phys. Rev. A* **1995**, *51*, 1431–1437.
- (4) Seideman, T.; Ivanov, M. Y.; Corkum, P. B. *Phys. Rev. Lett.* **1995**, *75*, 2819–2822.
- (5) Constant, E.; Stapelfeldt, H.; Corkum, P. B. *Phys. Rev. Lett.* **1996**, *76*, 4140–4143.
- (6) Cornaggia, C.; Salin, F.; Le Blanc, C. *J. Phys. B* **1996**, *29*, L749–L754.
- (7) Yu, H.; Zuo, T.; Bandrauk, A. D. *Phys. Rev. A* **1996**, *54*, 3290–3298.
- (8) Posthumus, J. H.; Codling, K.; Frasiniski, L. J.; Thompson, M. R. *Laser Phys.* **1997**, *7*, 813–825.
- (9) Thompson, M. R.; Thomas, M. K.; Taday, P. F.; Posthumus, J. H.; Langley, A. J.; Frasiniski, L. J.; Codling, K. *J. Phys. B* **1997**, *30*, 5755–5772.
- (10) Hishikawa, A.; Iwamae, A.; Hoshina, K.; Kono, M.; Yamanouchi, K. *Chem. Phys. Lett.* **1998**, *282*, 283–291.
- (11) Yu, H.; Zuo, T.; Bandrauk, A. D. *J. Phys. B* **1998**, *31*, 1533–1551.
- (12) Bandrauk, A. D.; Musaev, D. G.; Morokuma, K. *Phys. Rev. A* **1999**, *59*, 4309–4315.
- (13) Hishikawa, A.; Iwamae, A.; Yamanouchi, K. *J. Chem. Phys.* **1999**, *111*, 8871–8878.
- (14) Hishikawa, A.; Iwamae, A.; Yamanouchi, K. *Phys. Rev. Lett.* **1999**, *83*, 1127–1130.
- (15) Talebpour, A.; Bandrauk, A. D.; Yang, J.; Chin, S. L. *Chem. Phys. Lett.* **1999**, *313*, 789–794.
- (16) Iwamae, A.; Hishikawa, A.; Yamanouchi, K. *J. Phys. B* **2000**, *33*, 223–240.
- (17) Kou, J.; Zhakhovskii, V.; Sakabe, S.; Nishihara, K.; Shimizu, S.; Kawato, S.; Hashida, M.; Shimizu, K.; Bulanov, S.; Izawa, Y.; Kato, Y.; Nakashima, N. *J. Chem. Phys.* **2000**, *112*, 5012–5020.
- (18) Muller, A. M.; Uiterwaal, C. J. G. J.; Witzel, B.; Wanner, J.; Kompa, K. L. *J. Chem. Phys.* **2000**, *112*, 9289–9300.
- (19) Gridchin, V. V.; Popov, A. M.; Smirnova, O. V. *J. Exp. Theor. Phys.* **2001**, *93*, 295–300.
- (20) Tzallas, P.; Kosmidis, C.; Philis, J. G.; Ledingham, K. W. D.; McCanny, T.; Singhal, R. P.; Hankin, S. M.; Taday, P. F.; Langley, A. J. *Chem. Phys. Lett.* **2001**, *343*, 91–98.
- (21) Hishikawa, A.; Hasegawa, H.; Yamanouchi, K. *J. Electron Spectrosc.* **2004**, *141*, 195–200.
- (22) Miyazaki, K.; Shimizu, T.; Normand, D. *J. Phys. B* **2004**, *37*, 753–761.
- (23) Rajgara, F. A.; Krishnamurthy, M.; Mathur, D.; Nishide, T.; Shiromaru, H.; Kobayashi, N. *J. Phys. B* **2004**, *37*, 1699–1707.
- (24) Roithova, J.; Schroeder, D.; Schwarz, H. *J. Phys. Chem. A* **2004**, *108*, 5060–5068.
- (25) Schroeder, D. *Angew. Chem. Int. Ed.* **2004**, *43*, 1329–1331.
- (26) Chen, J.; Ma, R.; Ren, H.; Li, X.; Yang, H.; Gong, Q. *Int. J. Mass Spectrom.* **2005**, *241*, 25–29.
- (27) Zandee, L.; Bernstein, R. B. *J. Chem. Phys.* **1979**, *71*, 1359–1371.
- (28) Smith, D. J.; Ledingham, K. W. D.; Singhal, R. P.; Kilic, H. S.; McCanny, T.; Langley, A. J.; Taday, P. F.; Kosmidis, C. *Rapid Commun. Mass Spectrom.* **1998**, *12*, 813–820.
- (29) Castillejo, M.; Couris, S.; Koudoumas, E.; Martin, M. *Chem. Phys. Lett.* **1999**, *308*, 373–380.
- (30) Ledingham, K. W. D.; Smith, D. J.; Singhal, R. P.; McCanny, T.; Graham, P.; Kilic, H. S.; Peng, W. X.; Langley, A. J.; Taday, P. F.; Kosmidis, C. *J. Phys. Chem. A* **1999**, *103*, 2952–2963.
- (31) Shimizu, S.; Kou, J.; Kawato, S.; Shimizu, K.; Sakabe, S.; Nakashima, N. *Chem. Phys. Lett.* **2000**, *317*, 609–614.
- (32) DeWitt, M. J.; Peters, D. W.; Levis, R. J. *Chem. Phys.* **1997**, *218*, 211–223.
- (33) Castillejo, M.; Couris, S.; Koudoumas, E.; Martin, M. *Chem. Phys. Lett.* **1998**, *289*, 303–310.
- (34) Bhardwaj, V. R.; Vijayalakshmi, K.; Mathur, D. *Phys. Rev. A* **1999**, *59*, 1392–1398.
- (35) Talebpour, A.; Bandrauk, A. D.; Vijayalakshmi, K.; Chin, S. L. *J. Phys. B* **2000**, *33*, 4615–4626.
- (36) Holland, D. M. P.; Shaw, D. A.; Summer, I.; Bowler, M. A.; Mackie, R. A.; Shpinkova, L. G.; Cooper, L.; Rennie, E. E.; Parker, J. E.; Johnson, C. A. F. *Int. J. Mass Spectrom.* **2002**, *220*, 31–51.
- (37) Kong, X.; Luo, X.; Niu, D.; Li, H. *Chem. Phys. Lett.* **2004**, *388*, 139–143.
- (38) Hustrulid, A.; Kusch, P.; Tate, J. T. *Phys. Rev.* **1938**, *54*, 840–842.
- (39) Guilhaus, M.; Kingston, R. G.; Brenton, A. G.; Beynon, J. H. *Org. Mass Spectrom.* **1985**, *20*, 565–571.
- (40) Vekey, K.; Brenton, A. G.; Beynon, J. H. *J. Phys. Chem.* **1986**, *90*, 3569–3577.
- (41) Vekey, K.; Brenton, A. G.; Beynon, J. H. *Org. Mass Spectrom.* **1989**, *24*, 31–36.
- (42) Richardson, P. J.; Eland, J. H. D.; Lablanquie, P. *Org. Mass Spectrom.* **1986**, *21*, 289–294.
- (43) Bentley, T. W.; Wellington, C. A. *Org. Mass Spectrom.* **1981**, *16*, 523–526.
- (44) Dewar, M. J. S.; Holloway, M. K. *J. Am. Chem. Soc.* **1984**, *106*, 6619–6627.
- (45) Lammertsma, K.; Schleyer, P. v. R. *J. Am. Chem. Soc.* **1983**, *105*, 1049–1051.
- (46) Krogh-Jespersen, K. *J. Am. Chem. Soc.* **1991**, *113*, 417–423.
- (47) Zyubina, T. S.; Kim, G.-S.; Lin, S. H.; Mebel, A. M.; Bandrauk, A. D. *Chem. Phys. Lett.* **2002**, *359*, 253–261.
- (48) Zyubin, T. S.; Kim, G.-S.; Mebel, A. M.; Lin, S. H.; Bandrauk, A. D. *J. Theor. Comput. Chem.* **2003**, *2*, 205–231.
- (49) Weiner, B.; Williams, C. J.; Heaney, D.; Zerner, M. C. *J. Phys. Chem.* **1990**, *94*, 7001–7007.
- (50) Kompe, B. M.; Peel, J. B.; Traeger, J. C. *Org. Mass Spectrom.* **1993**, *28*, 1253–1261.
- (51) Schröder, D.; Loos, J.; Schwarz, H.; Thissen, R.; Roithova, J.; Herman, Z. *Int. J. Mass Spectrom.* **2003**, *230*, 113–121.
- (52) Angelova, G.; Novotny, O.; Mitchell, J. B. A.; Rebrion-Rowe, C.; Le Garrec, J. L.; Bluhme, H.; Seiersen, K.; Andersen, L. H. *Int. J. Mass Spectrom.* **2004**, *232*, 195–203.
- (53) Cameron, A.; Leszczynski, J.; Zerner, M. C.; Weiner, B. *J. Phys. Chem.* **1989**, *93*, 139–144.
- (54) Frisch, M. J.; Trucks, G. W.; Schlegel, H. B.; Scuseria, G. E.; Robb, M. A.; Cheeseman, J. R.; Montgomery, J. A., Jr.; Vreven, T.; Kudin, K. N.; Burant, J. C.; Millam, J. M.; Iyengar, S. S.; Tomasi, J.; Barone, V.; Mennucci, B.; Cossi, M.; Scalmani, G.; Rega, N.; Petersson, G. A.; Nakatsuji, H.; Hada, M.; Ehara, M.; Toyota, K.; Fukuda, R.; Hasegawa, J.; Ishida, M.; Nakajima, T.; Honda, Y.; Kitao, O.; Nakai, H.; Klene, M.; Li, X.; Knox, J. E.; Hratchian, H. P.; Cross, J. B.; Bakken, V.; Adamo, C.; Jaramillo, J.; Gomperts, R.; Stratmann, R. E.; Yazyev, O.; Austin, A. J.; Cammi, R.; Pomelli, C.; Ochterski, J. W.; Ayala, P. Y.; Morokuma, K.; Voth, G. A.; Salvador, P.; Dannenberg, J. J.; Zakrzewski, V. G.; Dapprich, S.; Daniels, A. D.; Strain, M. C.; Farkas, O.; Malick, D. K.; Rabuck, A. D.; Raghavachari, K.; Foresman, J. B.; Ortiz, J. V.; Cui, Q.; Baboul, A. G.; Clifford, S.; Cioslowski, J.; Stefanov, B. B.; Liu, G.; Liashenko, A.; Piskorz, P.; Komaromi, I.; Martin, R. L.; Fox, D. J.; Keith, T.; Al-Laham, M. A.; Peng, C. Y.; Nanayakkara, A.; Challacombe, M.; Gill, P. M. W.; Johnson, B.; Chen, W.; Wong, M. W.; Gonzalez, C.; Pople, J. A. *Gaussian 03*, revision C.02; Gaussian, Inc.: Wallingford, CT, 2004.
- (55) Becke, A. D. *Phys. Rev. A* **1988**, *38*, 3098–3100.
- (56) Becke, A. D. *J. Chem. Phys.* **1993**, *98*, 1372–1377.
- (57) Montgomery, J. A., Jr.; Frisch, M. J.; Ochterski, J. W.; Petersson, G. A. *J. Chem. Phys.* **1999**, *110*, 2822–2827.
- (58) Montgomery, J. A.; Ochterski, J. W.; Petersson, G. A. *J. Chem. Phys.* **1994**, *101*, 5900–5909.
- (59) Peng, C. Y.; Schlegel, H. B. *Isr. J. Chem.* **1993**, *33*, 449–454.
- (60) Gonzalez, C.; Schlegel, H. B. *J. Chem. Phys.* **1989**, *90*, 2154–2161.
- (61) Gonzalez, C.; Schlegel, H. B. *J. Phys. Chem.* **1990**, *94*, 5523–5527.
- (62) Hratchian, H. P.; Schlegel, H. B. *J. Chem. Phys.* **2004**, *120*, 9918–9924.